Supplementary material to: Nami HG, et al. S Afr J Sci. 2016;112(11/12), Art. #2016-0051, 12 pages.

How to cite: Nami HG, De la Peña P, Vásquez CA, Feathers J, Wurz S. Palaeomagnetic results and new dates of sedimentary deposits from Klasies River Cave 1, South Africa [supplementary material]. S Afr J Sci. 2016;112(11/12), Art. #2016-0051, 10 pages.
http://dx.doi.org/10.17159/sajs.2016/20160051/suppl

Sampling

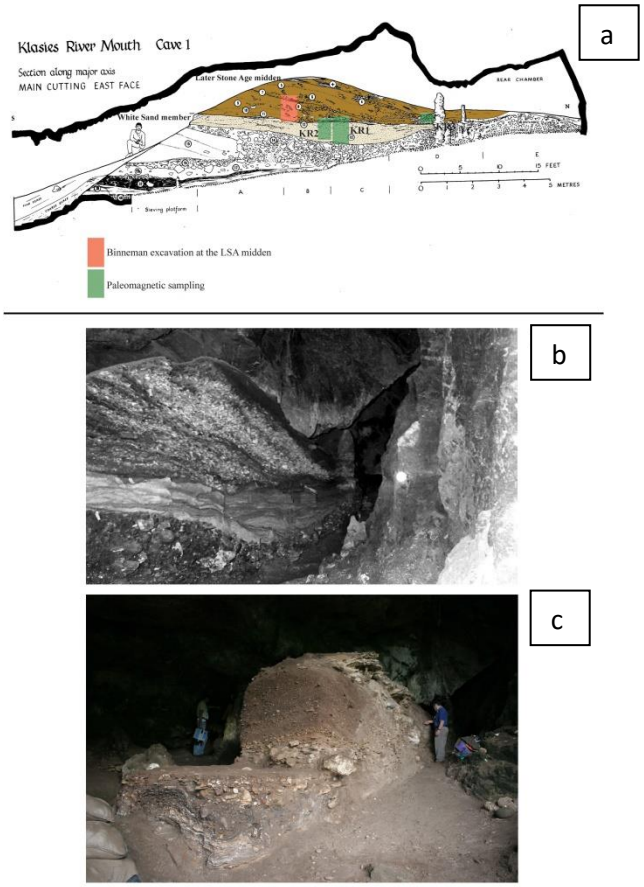

Source: Modified from Singer and Wymer[1]

Supplementary figure 1: (a) Singer and Wymer[1] stratigraphy with the different members mentioned in the text and the three palaeomagnetic samplings performed. The Binneman excavation is also highlighted. (b) Singer and Wymer's[1] picture of the Witness Baulk. Note the thickness of the LSA midden and how it thins out towards the back of the cave. (c) the Witness Baulk in May 2014 during the palaeomagnetic sampling.

Dating

Supplementary table 1: Previous OSL dates for the WS member

Sample	Age
	65 ka
UW272	67.4±6.6 ka

Source: Bada and Deems[2] and Feathers[3].

OSL

Methods

The samples were collected by driving light-tight containers into the profiles and capping the ends. About 30 mm of sediment from the ends was removed in the laboratory under red light and used for dose rate measurements. Except for a retained voucher, the rest was sieved to retrieve 180–210-µm grains, treated with HCl and H_2O_2, rinsed with water, separated from heavy minerals by immersion in 2.67 specific gravity lithium metatungstate, and etched with 48% HF for 40 min. Grains were mounted in specially designed single-grain disks for luminescence measurements.

Luminescence was measured on either a Risø TL–DA-15 or a Risø TL/OSL–DA-20 reader with single-grain attachments. Stimulation used a 532-nm laser delivering 45 W/cm^2. Detection was through 7.5-mm U340 (ultraviolet) filters. Each grain was exposed for 0.8 s at 125 °C. The first 0.06 s was used for analysis and the last 0.15 s for background. Heating at 240 °C for 10 s followed each dose, except for the calibrating test doses after which a 200 °C cut heat was employed. The test dose was about 5 Gy. Doses were delivered by a ^{90}Sr beta source which provided about 0.1 Gy/s to coarse-grained quartz.

Equivalent dose (D_e), which is a measure of the total absorbed dose through time, was determined using the single-aliquot regenerative dose (SAR) protocol.[4,5] The SAR method measures the natural signal and the signal from a series of regeneration doses on a single aliquot. The method uses a small test dose to monitor and correct for sensitivity changes brought about by preheating, irradiation or light stimulation. SAR consists of the following steps: (1) preheat, (2) measurement of natural signal (OSL or IRSL), L(1), (3) test dose, (4) cut heat, (5) measurement of test dose signal, T(1), (6) regeneration dose, (7) preheat, (8) measurement of signal from regeneration, L(2), (9) test dose, (10) cut heat, (11) measurement of test dose signal, T(2), (12) repeat Steps 6–11 for various regeneration doses. A growth curve is constructed from the L(i)/T(i) ratios and the equivalent dose is found by interpolation of L(1)/T(1). A zero regeneration dose and a repeated regeneration dose are employed to ensure the procedure is working properly.

An advantage of single-grain dating is the opportunity to remove from analysis grains with unsuitable characteristics by establishing a set of criteria which grains must meet. Grains were eliminated from analysis if they (1) had poor signals (as judged from errors on the test dose greater than 30% or from net natural signals not at least three times above the background standard deviation), (2) did not produce, within 20% (usually about 2σ), the same signal ratio (often called recycle ratio) from identical regeneration doses given at the beginning and end of the SAR sequence, suggesting inaccurate sensitivity correction, (3) yielded natural signals that did not intersect saturating growth curves, (4) had a signal larger than 10% of the natural signal or a signal not distinguishable from background after a zero dose, (5) produced a zero D_e (within 1σ of zero), or (6) contained feldspar contaminates (judged visually on growth curves by a reduced signal from infrared stimulation before the OSL measurement; done on two doses to lend confidence that the reduction in signal is a result of feldspar contamination).

A dose recovery test was performed on some grains. The luminescence of the grains is first removed by exposure to the laser (using the same parameters mentioned earlier). A dose of about 60 Gy was administered and treated as an unknown. The SAR procedure was then applied. Successful recovery is an indication that the procedures are appropriate.

A D_e value was obtained for each suitable grain. Because of varying precision from grain to grain, the same value will not obtained for each grain even if all are of the same age. Instead, a distribution is produced. The central age model[6] was used in evaluation of D_e distributions. The central age model, instead of assuming a single true value, assumes a normally distributed natural distribution of D_e values, even for single-aged samples, because of non-statistical sources of variation. The central age is the mean of that distribution and the standard deviation is the over-dispersion (σ_b), which represents that deviation beyond what can be accounted for by measurement error. A finite mixture model was also applied.[6] The model uses maximum likelihood to separate the grains into single-aged components based on the input of a given σ_b value and the assumption of a log-normal distribution of each component. The model estimates the number of components, the weighted average of each component, and the proportion of grains assigned to each component. The model provides two statistics for estimating the most likely number of components: maximum log likelihood (llik) and Bayes information criterion (BIC). The finite mixture model is appropriate for samples that have been post-depositionally mixed (although with limitations).

Dose rate was determined by thick source alpha counting, beta counting and flame photometry. Moisture content was measured at 7.7±3 % and used in the analysis. Cosmic dose rate was negligible after taking account of the mountain over-burden[5] and of the fact that the samples were drawn from near the back of the cave. Radioactivity concentrations were translated into dose rates following Guérin et al.[7]

Age was calculated using a laboratory constructed spreadsheet based on Aitken[8]. All given error terms are computed at 1σ. The year 2015 is the reference point for ka (thousands of years ago).

Results

Dose rate

Supplementary table 2 gives the relevant radionuclide concentrations. The beta dose rate calculated from these concentrations is compared with that measured directly by beta counting, which is given in Supplementary table 2. There are no significant differences that might be caused, for example, by U-Th disequilibrium in the U decay chain. Supplementary table 3 gives the estimated dose rates, which are similar for both samples, but slightly more than the dose rate of the previous sample (0.78±0.06).[7]

Supplementary table 2: Radioactivity

Sample	^{238}U (ppm)	^{233}Th (ppm)	K (%)	Beta dose rate (Gy/ka)	
				ß-counting	α-counting/flame photometry
UW3113	2.13±0.14	2.91±0.69	0.29±0.01	0.64±0.06	0.63±0.03
UW3114	1.05±0.11	5.89±0.96	0.42±0.01	0.64±0.07	0.66±0.03

Supplementary table 3: Dose rates (Gy/ka)

Sample	Alpha	Beta	Gamma	Cosmic	Total
UW3113	0.01±0.01	0.48±0.03	0.41±0.04	0.01±0.01	0.90±0.05
UW3114	0.01±0.01	0.52±0.03	0.46±0.05	0.01±0.01	0.99±0.05

Equivalent dose

Supplementary table 4 gives the number of grains measured, the number rejected using the criteria listed earlier, and the number accepted. The samples showed relatively high luminescence sensitivity for quartz. The acceptance rate for signals from which an equivalent dose could be measured averaged 13.1%. This is an average over two readers, one of which is more sensitive than the other.

Supplementary table 4: Acceptance rates

Sample	*N*[†]	No signal	Recycle	Too high	Recuperation	Feldspar	Zero dose	Accepted	Rate (%)
UW3113	962	680	68	48	4	13	3	146	15.2
UW3114	967	753	53	37	0	10	8	106	11.0
Total	**1929**	**1433**	**121**	**85**	**4**	**23**	**11**	**252**	**13.1**

[†]*N refers to the number of grains measured; no signal refers to grains that had no measurable signal; recycle refers to the number of grains rejected for failing the recycle test and for no other reason; too high refers to natural signals higher than the signal from the highest regeneration point; recuperation refers to significant signal after zero dose and preheat; feldspar refers to feldspar contaminated as detected by sensitivity to IRSL; zero dose refers to grains rejected because the equivalent dose was not significantly different from zero.*

A dose recovery test was conducted on 191 grains from both samples, of which 31 passed all the acceptance criteria. The central tendency of the derived/administered (~60 Gy) ratio, from the central age model, is 1.04±0.09, which is satisfactory. The over-dispersion of the ratio distribution is 35±8%, which is a measure of intrinsic variation as a result of machine and sample factors and which can be taken as the minimum over-dispersion expected for a single-aged sample. This is higher than average. A value of 30% was taken as typical for a single-age sample when evaluating age distributions.

Supplementary table 5 gives the equivalent dose from the central age model[3] and the over-dispersion for each sample. The over-dispersion is not much higher than the 30% assumed for a single age sample. A finite mixture model was applied to divide the sample into single-value components. All grains of UW3114 fell into a single component, while UW3113 split into two components, one of which (at 60.2±2.6 Gy) contained 93.7% of the grains. Matters did not change much if the assumed over-dispersion for a single-aged sample was reduced to 20%. UW3113 still divided into two components, one at 60.4 Gy for 92.8 % of the grains. UW3114 also divided into two components, which were about equally distributed (55% and 45%). With no reason to prefer one over the other, the central age is still the best estimate. Supplementary table 6 gives the ages.

Supplementary table 5: Equivalent dose (central age model)

Sample	*N*	Equivalent dose (Gy)	Over-dispersion (%)
UW3113	146	54.5±2.8	45.3±4.5
UW3114	106	55.7±2.9	36.5±4.8

Supplementary table 6: Ages

Sample	Age (ka)	Error (%)	Basis
UW3113	66.5±4.8	7.2	93.7% component
UW3114	56.3±4.6	8.2	Central age model

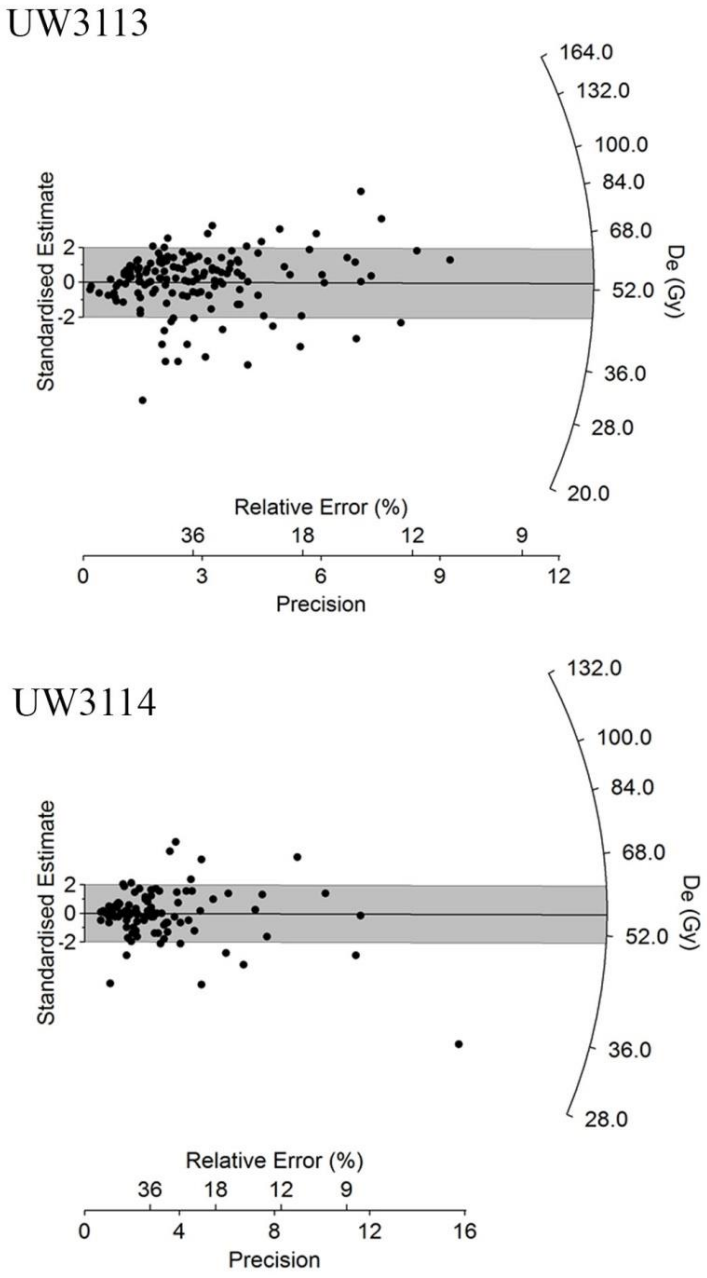

Supplementary figure 2: Radial graphs of each sample. A radial graph plots precision against the equivalent dose, standardised to the number of standard errors from which the value is to a reference point. The reference point in both graphs is the equivalent dose value obtained from the central age model. Shaded areas encompass all points within two standard errors of the reference. Lines drawn from the origin through any point intersect the right-hand scale at the estimated equivalent dose.

Palaeomagnetic study

Supplementary table 7: Percentage difference of susceptibility with frequency χ_{fd} %= 100 x [(χ_{f1} - $\chi_{f2,3}$) / χ_{f1}]. The f1 frequency is near 1000 Hz, f2 near 4000 Hz and f3 near 16 000 Hz.

RM sample	Depth (cm)	χfd%f1f2	χfd%f1f3	χfd%f2f3
1	6	7.13	13.02	6.34
2	9–10	8.26	14.55	6.86
3	17.5	7.78	12.15	4.74
4	30–31	6.19	10.51	4.60
5	36–39	7.12	13.85	7.24
6	44–45	7.92	14.14	6.76
7	49–50	6.70	11.22	4.85
8	55	6.04	11.73	6.05
9	60	7.77	10.84	3.34
10	65	5.63	6.27	0.68
11	70	7.92	14.14	6.76
12	79	4.97	8.97	4.22

Supplementary table 8: Directions of secondary components that recorded a normal GMF position, virtual geomagnetic pole positions, intervals of each sample and maximum angular deviations

Sample	Declination	Inclination	Longitude	Latitude	Intervals of selected direction	Maximum angular deviation
KR1 5	14	-42	79	74	0–15	4.2
KR1 32	348	-54	288	80	0–50	4.7
KR2 9	12.2	-68	181	71	0–25	8.6
KR3 5	68	-49	130	33	0–15	5.1

Note: Negatives values show negative inclination. Intervals of selected ChRM are given in mT.

Supplementary table 9: Characteristic remanent magnetisation, virtual geomagnetic pole positions, intervals of each sample and maximum angular deviations

KR1							
Sample	**Depth (cm)**	**Declination**	**Inclination**	**Longitude**	**Latitude**	**Int.ChRM**	**Maximum angular deviation**
1	0	36	-13	83	47	9–30	2.2
2	1.5	27	-65	157	68	0–30	1.6
3	3	352	-50	318	82	9–30	1.9
4	4.5	359	-57	217	86	6–30	1.1
5	5.5	299	-19	303	280	15–Or.	4.6
6	6.5	17	-39	80	71	12–30	1.0
7	7.5	7	-67	188	74	9–30	0.6
8	9	346	-56	278	78	9–Or.	2.6
9	10.5	16	-46	93	75	6–Or.	3.0
10	17.5	5	-69	195	71	3–30	4.2
11	18.5	18	-57	133	75	3–50	2.7
12	20.5	256	-51	261	7	3–30	4.0
13	22	59	-67	153	45	20–Or.	7.5
14	23	19	-54	121	74	0–30	1.0
15	24	38	-41	107	55	20–80	6.8
16	25.5	359	-55	233	88	3–50	3.4
17	30	20	-54	122	73	0–50	5.6
18	34	10	-40	65	76	9–50	6.8
19	36	10	-52	107	82	0–80	2.3
20	42	20	-52	115	73	3–60	1.2
21	42.5	41	-47	116	55	6–25	4.3
22	43.5	43	-72	166	53	0–60	8.2
23	44.5	32	-48	113	62	12–50	6.9
24	46	12	-59	148	79	0–60	2.9
25	47.5	356	-64	218	78	15–50	3.3
26	49.5	9	-65	179	75	0–50	3.0
27	50.5	345	-67	235	71	0–40	2.4
28	52	357	-54	283	87	0–80	9.8
29	54	352	-50	318	83	9–40	7.8
31	61.5	67	-35	119	29	12–Or.	8.0
32	63	304	62	347	-3	50–Or.	9.0
33	64.5	314	-87	210	38	3–40	2.7
34	66	348	-57	271	80	3–30	1.9
35	67	21	-53	118	79	0–30	8.9
36	68.5	20	-58	136	73	0–40	9.7
37	70	342	-60	263	74	0–30	2.7
38	71.5	341	-61	260	73	0–40	4.9
39	72.5	3	-54	126	87	0–40	2.7
40	73.5	354	-61	233	81	0–50	1.7
41	75	353	-56	269	84	12–100	4.4
42	77	20	-70	175	66	0–30	2.2
43	79	4	-50	71	85	0–30	2.8

Suppl. table 9 continues on p.9

KRM2							
Sample	**Depth**	**Declination**	**Inclination**	**Longitude**	**Latitude**	**Int.ChRM**	**Maximum angular deviation**
3	8	316	-65	259	55	0–30	5.0
4	9	9	-46	76	80	0–30	1.5
5	9.5	327	68	4	0	6–30	8.5
6	11	346	-41	331	74	3–50	2.5
7	12	185	48	246	-83	0–80	2.8
8	13	40	-69	160	56	9–6O	6.3
9	15	121	27	119	-33	25–120	4.7
10	16	35	22	67	34	0–80	3.3
11	17.5	349	-40	341	75	3–25	5.4
12	19	304	-46	286	42	0–80	5.9
13	20.5	271	12	300	-3	12–30	7.9
14	28.5	13	-53	115	79	0–40	8.9
15	30	24	-10	67	53	6–50	5.3
16	31.5	31	-55	126	65	0–30	8.5
17	33	22	-67	165	68	0–50	7.0
18	35	15	-52	112	77	0–80	1.5
19	37	354	-52	309	85	0–30	4.3
20	44.5	64	-55	135	38	0–50	5.0
21	47	53	-77	176	46	0–60	1.8
22	48.5	6	-59	166	83	0–50	2.8
23	51	9	-58	149	81	0–50	3.2
24	52.5	18	-44	91	72	3–30	7.8
25	54	7	-84	202	46	12–25	1.9
26	60.5	10	-48	86	80	0–50	2.9
27	62	6	-36	46	75	15–60	2.3
28	63.5	354	-47	341	82	0–50	1.8
29	66	12	-48	91	79	15–50	2.0
30	68	11	-48	89	79	0–60	4.1
KRM3							
Sample	**Depth**	**Declination**	**Inclination**	**Longitude**	**Latitude**	**Int.ChRM**	**Maximum angular deviation**
1	3	58	-13	101	30	0–30	4.5
2	4.5	74	-34	122	23	3.30	8.0
3	5.5	71	-23	114	22	3.30	7.0
5	7.5	348	-35	345	72	15–30	5.0
6	9	351	10	10	50	20–80	9.7
7	11	229	50	304	-49	60–80	2.6
8	12	20	-42	90	70	6–50	4.8

Note: Negatives values show negative inclination or VGP located in the southern hemisphere.

Int.ChRM, Intervals of selected ChRM (in mT); Or., origin in the Zijderveld diagram

Supplementary table 10: Site mean direction and the difference with the IGRF directions

Site/samples	*N*	Declination (D°)	Inclination (I°)	D° – IGRF difference	I° – IGRF difference	k	R	A95
KR1	42	8.6	-56.8	35.74	7.75	9.48	37.67	7.6
KR1 6-31	25	15.0	-58.1	42.14	6.45	17.44	23.62	7.1
KR2	28	7.99	-50.1	35.13	14.45	3.14	19.41	14.93
KR2 14-30	19	9.88	-53.79	37.02	10.76	15.19	17.82	8.9

A95, semi-angle of cone 95% confidence; k, Fisher's precision parameter; R, resultant vector

References

1. Singer R, Wymer J. The Middle Stone Age at Klasies River Mouth in South Africa. Chicago, IL: University of Chicago Press; 1982.
2. Bada JL, Deems L. Accuracy of dates beyond ^{14}C dating limit using the aspartic acid racemisation reaction. Nature. 1975;255:218–219. http://dx.doi.org/10.1038/255218a0
3. Feathers JK. Luminescence dating in less than ideal conditions Case studies from Klasies River main site and Duinefontein, South Africa. J Archaeol Sci. 2002;29:177–194. http://dx.doi.org/10.1006/jasc.2001.0685
4. Murray AS, Wintle AG. Luminescence dating of quartz using an improved single-aliquot regenerative-dose protocol. Radiat Meas. 2000;32:57–73. http://dx.doi.org/10.1016/S1350-4487(99)00253-X
5. Wintle AG, Murray AS. A review of quartz optically stimulated luminescence characteristics and their relevance in single-aliquot regeneration dating protocols. Radiat Meas. 2006;41:369–391. http://dx.doi.org/10.1016/j.radmeas.2005.11.001
6. Galbraith RF, Roberts RG. Statistical aspects of equivalent dose and error calculation and display in OSL dating: An overview and some recommendations. Quat Geochronol. 2012;11:1–27. http://dx.doi.org/10.1016/j.quageo.2012.04.020
7. Guérin G, Mercier N, Adamiec G. Dose-rate conversion factors: Update. Ancient TL. 2011;29:5–8.
8. Aitken MJ. Thermoluminescence dating. London: Academic Press; 1985. http://dx.doi.org/10.1016/0735-245X(85)90003-1